 https://doi.org/10.3311/PPch.21889

Periodica Polytechnica Chemical Engineering, 67(3), pp. 460–471, 2023

Elucidation on Performance and Structural Properties of Skinned Asymmetric Nanofiltration Membrane Based on Theoretical Models

Sabariah Rozali[1], Nurul Hannan Mohd Safari[1], Abdul Rahman Hassan[1,2*], Roslan Umar[1]

[1] East Coast Environmental Research Institute, Universiti Sultan Zainal Abidin, 21300 Kuala Nerus, Terengganu, Malaysia
[2] Faculty of Industrial Design & Technology, Universiti Sultan Zainal Abidin, 21300 Kuala Nerus, Terengganu, Malaysia
* Corresponding author, e-mail: rahmanhassan@unisza.edu.my

Received: 19 January 2023, Accepted: 09 May 2023, Published online: 01 June 2023

Abstract

In this study, the performance and structural properties of enhanced skinned asymmetric nanofiltration (NF) membranes were experimentally and theoretically analyzed. Based on Donnan and steric-hindrance transport mechanism, the relationship of performances and key properties of the fabricated nanofiltration membranes were examined. At the optimum concentration of polymer, the skinned nanofiltration membranes achieved high salt rejection up to 85% and high solutes separation efficacy. Moreover, morphological and modeling analysis discovered that, the optimum membranes produced good pore size and fine key properties with 1.20 nm of pore radius, 4.96 μm of ratio of thickness to porosity ($\Delta x/A_k$) and −1.56 of surface charge, ζ as well as uniform pore size distributions. The findings from this study proved that the strategic utilization and manipulation of good membranes material is a simple and good attempt to upgrade the membranes capability and usability which lead towards the application in various membrane separation processes.

Keywords

nanofiltration, modeling, key properties, structural details, pore size distribution

1 Introduction

Membrane technology has gained widespread attention for various separation applications such as from microfiltration, ultrafiltration, nanofiltration, reverse osmosis and also gas separation. There are several procedures that can be used in membranes fabrication such as phase inversion, non-solvent induced phase separation (NIPS), and thermal-induced phase separation (TIPS) [1].

Phase inversion technique is the most commonly used in making asymmetric membranes. Phase inversion is initiated as immersion precipitation occurred when polymer is cast onto a suitable substrate and then submerged in a coagulation fluid. The interchange of solvent and non-solvent in phase inversion will generate an asymmetric membrane with a denser top layer and also have very thin more or less dense skin reinforced by a porous sub-layer [2, 3].

A skinned, thin and dense asymmetric nanofiltartion (NF) membrane could be prepared by using dry/wet phase inversion technique [4, 5]. In this technique, the formation of fine skinned membranes depends on two major factors of kinetic and thermodynamic factors which including of interactions between solvents and polymers, interactions between solvents and non-solvents, interfacial stability, solvent de-mixing rate [6–9]. Polymers like polyvinylidene fluoride (PVDF), cellulose acetate (CA), polysulfone (PSf), polyethersulfone (PES) have been used for the making asymmetric membranes due to their good thermal stability, outstanding oxidative and good mechanical strength [10, 11].

In addition, the used of different membranes materials enabling the making of membranes with a wide range of varied pore sizes that maybe used in numerous of modules and configurations for many industries like gas separation, water purification, medicinal treatments, wastewater treatment and biotechnology [12–14].

1.1 Nanofiltration membranes

NF membranes are utilized not only to separate aqueous solutions containing electrolytes but also for separation of uncharged solute with size range of about 1–10 nm. Basically, NF membranes are used for separation of solutes and salts based on their unique properties. Besides, it also used as a pre-treatment in the desalination process as NF allows diffusion to occur on certain monovalent ions such

Cite this article as: Rozali, S., Mohd Safari, N. H., Hassan, A. R., Umar, R. "Elucidation on Performance and Structural Properties of Skinned Asymmetric Nanofiltration Membrane Based on Theoretical Models", Periodica Polytechnica Chemical Engineering, 67(3), pp. 460–471, 2023.
https://doi.org/10.3311/PPch.21889

as sodium and chloride. Thus, for more complex molecules and multivalent ions are highly retained [15].

Rapid growth on industrial interest and demand for NF membranes are driven by the dual factors of steric hindrance and Donnan factors as transport mechanism for the efficient separation capability [16–20]. NF has been widely used in applications namely in the production of drinking water and also water treatment. NF has been applied in treatment of water including ground, surface and effluent water because of its ability to remove organic and particle impurities [21]. According to the recent literature, the NF process has been applied as a new approach in agricultural manufacturing process, focusing on concentrating plants extract for commercial use in pharmaceutical and food industries [22].

1.2 Transport mechanism and modeling

In generally, NF membranes possess of negative charge, and the separation process will be occurred in according to the different magnitudes of signs and valences for the different membranes process separation performance under specific assumptions which derived by the established irreversible thermodynamic model [4, 23]. A steric hindrance factor actually is a transport mechanism which could be explained as the comparison of solutes size and membranes pores. The larger solutes will be rejected and allow the smaller ones to be permeated easily through the membranes. Meanwhile, the Donnan effect referred to the charge interactions of ions and the membrane [1].

Therefore, transport models were applied to identify the structural characteristics, electrostatic characteristics, and transportation processes of NF membranes. These models are relied on mass transport mechanisms such as diffusion, adsorption, concentration polarization, ion exchange or others. So each model has been developed for a particular set of circumstances. Based on steric hindrance pore (SHP) model and Teorell-Meyer-Sievers (TMS) model, certain presumptions have been made. For example, these models are used to define partitioning effects as membrane is assumed a charged porous layer. Besides, the extended Nernst-Planck equation is used to calculate mass transfer through the membrane. These presumptions will be useful to calculate a membrane's attributes [24]. In addition, the data on the transport of a solvent or solute via NF membranes can be evaluated using the Spiegler-Kedem model [25].

Based on the previous reports, these SHP, TMS and Spiegler-Kedem theoretical models were applied in the experiments to determine the optimum performance of NF membrane in terms of key properties like pore radius (r_p), surface charge (ζ) and pore size distribution [26, 27]. Furthermore, TMS model also applied to calculate the reflection coefficient, (σ) in the single salt solution experiments. This is important in order to investigate the rejection behavior of salt solution [28, 29].

It is well recognized that the skin active layer determined the amount of solutes permeate from the membranes. This transport of these solutes was driven by the characteristics of membranes morphology, pore size, charge density and skin active layer [30]. The ions separation can be revised by the improvement in membrane efficacy [31].

In addition to design factors, fabrication parameters are also crucial to the characteristics of the produced membrane [1]. For example, the influence of PES as polymer concentration in fabrication of membrane led to the inducing of chain entanglement and therefore reduced the microvoid concentration in the skin layer [32, 33]. Therefore, the rights choose on materials, including polymers, solvents, and non-solvents, when creating asymmetric membranes really need to be considered [34].

As the polymer concentrations factors had been reported affect the membranes separation performance, its significant effects on the membranes properties and structural details are not fully evaluated. Moreover, the use of modeling technique and pore size distribution analysis to explain the factor of polymer concentrations on membrane performance-properties is not fully addressed. Therefore, the relationships between the composition of polymer material and performance-properties induced by enhanced membranes parameters and structural details of skinned NF membranes were experimentally studied and modeled.

2 Experimental

2.1 Materials

The polyethersulfone (PES, Radel A300) and N-methyl-2-pyrrolidone used as raw materials. Methanol and water were used as a post-treatment media. For the solute separation test, the neutral solutes of glycerol, glucose, saccharose, raffinose and PEG 1000 (Sigma Aldrich) were employed [35]. Besides, monovalent salt (NaCl) and multivalent salts ($MgCl_2$, Na_2SO_4 and $MgSO_4$) were used to evaluate the membranes performance.

2.2 Dope formulations and membrane making

A polymer/solvent/non-solvent ternary dope component was carried out through a turbidimetric titration method at room temperature and 84% humidity [8]. In this method, 100 g of polymer solution was titrated with distilled water

until the dope converted into a milky solution. Then, the dope formulation was measured as tabulated in Table 1. Based on these formulations, the membranes dopes (500 ml) were prepared using dope apparatus.

Prior to casting, the membranes dope was then placed into ultrasonic bath for 6 hours to remove air bubbles and degassing purpose. Subsequently, the membranes were cast on a glass plate using auto-casting machine at room temperature (30 °C). The membranes thickness was fixed at 150 μm. Then, the membranes were dipped into water bath (coagulation media) for 24 hours. For the post treatment process, membranes were dipped into n-hexane and ethanol for 6 and 24 hours, respectively. Finally, the treated membranes were dried for 24 hours at room temperature before it ready to be used in the nanofiltration test.

2.3 Membrane performance

NF membranes samples were undergo a compaction test at 500 kPa for 1 hour. 20 mL of permeate samples were collected for each three independent experiment run and weighed minutely by an electronic balance. The salts concentration in feed and permeate stream were measured using a conductivity meter (Model Hach SENSION5). The solutes rejections were examined for fluxes and real rejection at a pressure of 500 kPa using a Millipore permeation cell with membranes area of about 1.39×10^{-3} m^2. The measurements of the neutral solutes were conducted using a Total Organic Carbon (TOC) Analyzer from Thermo Scientific.

In this study, the Scanning Electron Microscopy (JEOL JSM 6360LA) was used to analyze the membranes morphologies. For this analysis, the membrane samples were cryogenically ruptured after being placed in nitrogen liquid for a brief period of time for morphological study. The broken samples were placed cautiously on stubs and covered with a gold layer. The membranes samples were scanned using 600X–2500X magnification and 10.0 kV potentials under a microscope. Moreover, the pore size distribution analysis was conducted using neutral solutes rejection data and MiniTAB® statistical software [36, 37].

Table 1 Multi components dope solution formulations

Membrane	PES (wt%)	NMP (wt%)	Water (wt%)
NF17	17.26	72.21	10.53
NF19	18.91	71.03	10.06
NF21	20.42	70.06	9.52
NF23	22.71	68.74	8.55
NF25	25.26	67.38	7.36

2.4 Membrane characterizations and modeling

2.4.1 Permeation of fluxes

Permeation of fluxes data were evaluated based on the following equation (Eq. (1)) [1]:

$$J_v = \frac{V}{A \times \Delta t}. \tag{1}$$

2.4.2 Real rejection, R_{real}

The NF membranes separation capability was evaluated as follows [38]:

$$R_{real} = \left(1 - \frac{C_p}{C_w}\right) \times 100. \tag{2}$$

2.4.3 Spiegler-Kedem and Steric-Hindrance Pore (SHP) model

Based on these models, the transports element in NF membranes is mainly driven by diffusion and convection. The separation properties of NF membranes and process are well-described by the following equations (Eqs. (3) to (13)) [38, 39]. The used of these equations for determining the membranes parameters was described elsewhere as in our previous report [26]:

$$J_s = -P\Delta x \frac{dc}{dx} + (1-\sigma) J_v c, \tag{3}$$

$$J_v = \frac{\varepsilon r}{8\eta\tau} \frac{\Delta P}{\Delta x}, \tag{4}$$

$$R_{real} = \left(\frac{\sigma(1-F)}{1-\sigma F}\right), \tag{5}$$

$$F = \exp\left(-\frac{1-\sigma}{P} J_v\right), \tag{6}$$

$$\sigma = 1 - H_F S_F, \tag{7}$$

$$P_s = H_D S_D D_s \left(\frac{A_k}{\Delta x}\right), \tag{8}$$

$$A_k = \frac{1}{S_D H_D}, \tag{9}$$

$$H_F = 1 + \frac{16}{9}\eta^2, \tag{10}$$

$$H_D = 1, \tag{11}$$

$$S_F = (1-\eta)^2\left[2-(1-\eta)^2\right], \tag{12}$$

$$S_F = (1-\eta)^2, \tag{13}$$

where:

$$\eta = \frac{r_s}{r_p}. \tag{14}$$

The combination of Spiegler-Kedem and SHP model allowed the determination of membranes structural parameters such as reflection coefficient, (σ), pore radius, (r_p), solutes permeability (P_s), ratio of thickness to porosity ($\Delta x/A_k$) and the important steric-hindrance parameters (H_F, H_D, S_F and S_D) [26, 40].

2.4.4 Teorell-Meyer-Sievers (TMS) Model

This model was used to quantify and describe the electrostatic properties. This model implies the fixed circular dispersion of charges and ions that occurs in membrane electrical characteristics for determination of the Donnan parameters such as reflection coefficient of salt, (σ_{salt}), salt permeability (P_{salt}), charge density, (X_d) and the membrane surface charge, (ζ) [41]. The derived equations to estimate the electrostatic properties were previously discussed in our report [26].

3 Result and discussion

3.1 Membranes performance and separation capability

In order to fabricate high performances membranes, turbidimetric titration measurement was used to determine the compositions in all cases. The dope solutions' compositions were collated as shown in Table 1.

Variations in the polymer concentration in the dope solution result in various membrane structures with various membrane properties. Additionally, the optimum polymer concentration must be taken into account as demonstrated that at these optimum polymer concentration, dope solution starts to exhibit noticeable chain entanglement. The pure water permeation (PWP) of the prepared NF membranes was depicted as in Fig. 1.

The symbols represent average of three experiments run, in which error bars represented the standard deviation. The error bars are not visible when they are smaller than the size of symbols in the graph as also reported by other researchers [42–44]. The membranes permeability can be interpreted directly from PWP data whereas the compressibility data can be evaluated based on the water flux changes

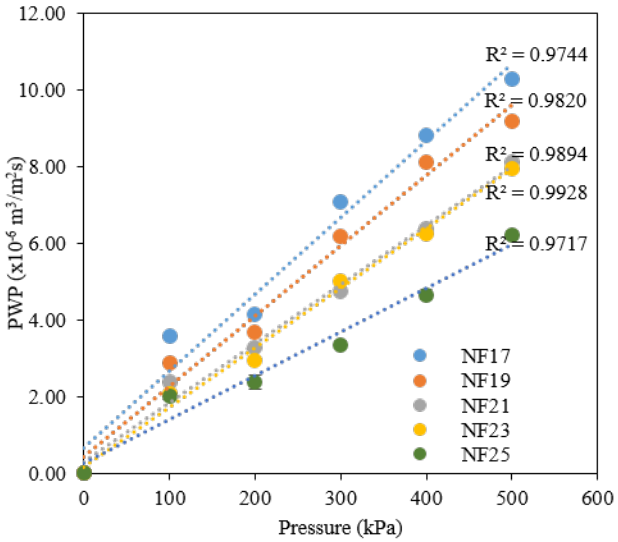

Fig. 1 PWP of skinned NF membranes. Error bars represent the standard deviation and not shown when they are smaller than size of symbols

with times. Meanwhile, membranes volume flux and salt rejection were depicted as in Figs. 2 and 3, respectively.

From Fig. 2, the increasing in operating pressure caused the higher membranes fluxes. At lower polymer concentration of NF19 membranes exhibited higher flux. However, there are not many changes in terms of volume flux between these membranes over the pressure range. At 450–500 kPa, the highest flux of about 4.08×10^{-6} m^3/m^{2}s was performed by NF19 membrane. This may be the result of the membrane skin layer porosity which is the more porous membranes lead to more productivity.

In comparison, the obtained volume fluxes are found to be comparable to the market available membranes such as NF-45 and AFC 30 (7.0×10^{-6} m^3/m^{2}s at 500 kPa) [45–47]. Fig. 3 demonstrates that as pressure increased, more NaCl was rejected. The membranes displayed higher salt rejection at high polymer concentrations (> 20 wt%). Membranes performances in Fig. 2 and Fig. 3 showed that the increasing of polymer in dope solution produced a thicker, denser skin layer that encouraged the development of more selective membranes. In contrast, casting membranes with low polymer concentration produced a thin, porous skin layer that had a high degree of permeability and low separation performances. This outcome was consistent with earlier proved study [48].

Fig. 4 showed the fluxes and salt rejection of skinned membranes. It was clearly observed that there is an intersection of membranes performances closed to the polymer concentration of 20.42 wt%. At this point, the fabricated membrane showed moderate performance. Although the rejection increased, the membranes volume flux was found

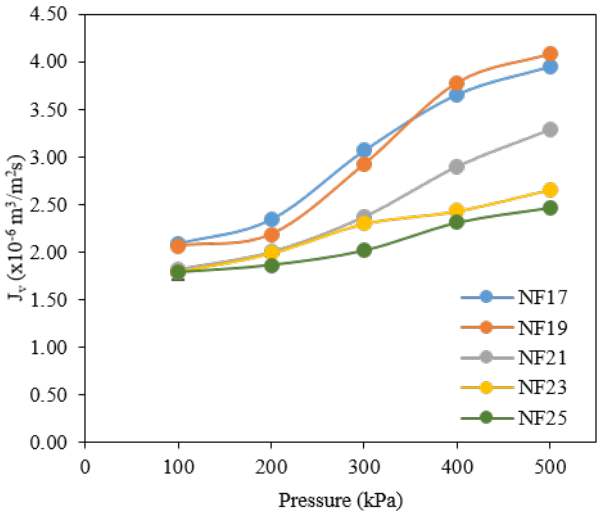

Fig. 2 Volume fluxes of 0.01 M NaCl. Error bars represent the standard deviation and not shown when they are smaller than size of symbols

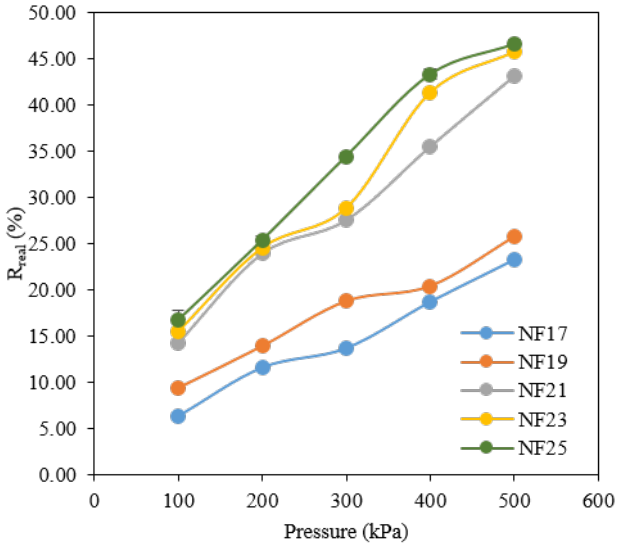

Fig. 3 Real rejection, R_{real} of 0.01 M NaCl. Error bars represent the standard deviation and not shown when they are smaller than size of symbols

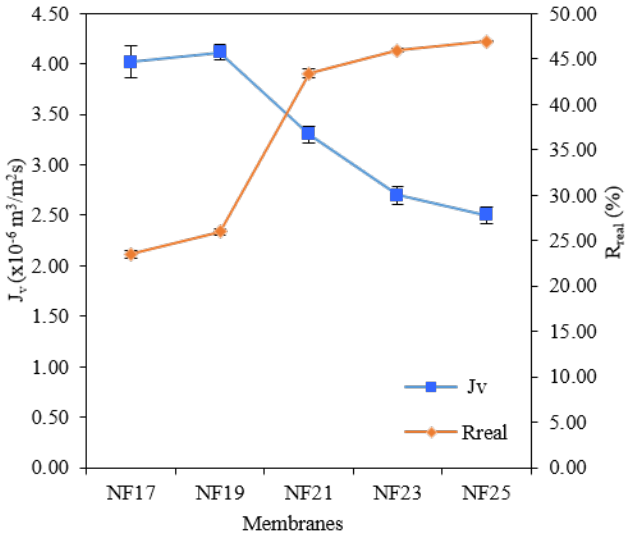

Fig. 4 J_v and R_{real} of 0.01 M NaCl at 500 kPa. Error bars represent the standard deviation and not shown when they are smaller than size of symbols

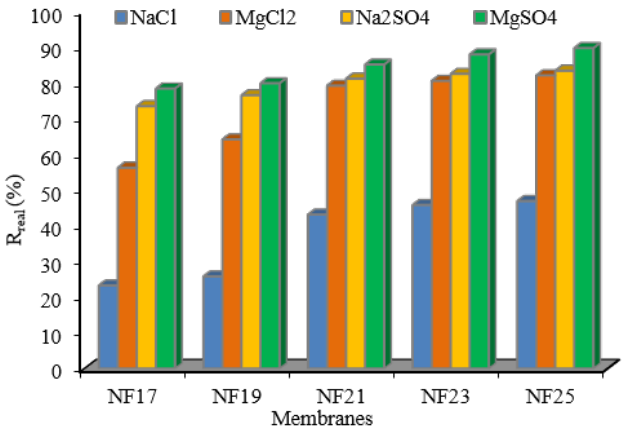

Fig. 5 Salts real rejection, R_{real} of 0.01 M at 500 kPa

reduced beyond this point. As a result, the polymer concentration of 20.42 wt% can be regarded as the optimum polymer concentration based on the performance trends.

In Fig. 5, the rejection results of multivalent salts (Na_2SO_4, $MgSO_4$, $MgCl_2$ and NaCl) at 500 kPa of operating pressure were plotted. It can been that the increment in polymer concentration affected the rejection performances. In a sequence of rejection performances of $MgSO_4$ > Na_2SO_4 > $MgCl_2$ > NaCl, high polymer concentration (>20 wt%) demonstrated of high salt rejection more than 85%).

Table 2 demonstrates that the solute size followed the order of Mg^{2+} > SO_4^{2-} > Na^+ > Cl^-, whereas the ion diffusivity (D) follows the sequences of Cl^- > Na^+ > SO_4^{2-} > Mg^{2+}. The trends may assist in comprehending how the real rejection in Fig. 5 was acquire. The solutes transports through the NF membranes are strongly influenced by diffusivity and size. The Donnan concept states that a higher valence counter-ion results in less in salt rejection [49, 50].

Table 2 Solute size and diffusion coefficient for ions

Ions	r_s (nm)	$D_\infty \times 10^{-9}$ (m^2/s)
Na^+	0.18	1.33
Mg^{2+}	0.35	0.7
Cl^-	0.12	2.01
SO_4^{2-}	0.23	1.06

3.2 Membrane parameters and structural properties

In this study, different types of uncharged/neutral solutes of different series of molecular weight, diffusivities

and solutes are listed in Table 3. These solutes are very famous and commonly used as solutes maker by numerous researchers for NF experiment [51, 52]. In Table 3, the average values of $\Delta x/A_k$ were determined based on the modeling analysis using Eqs. 9 and 10 which taken into account if the reflection coefficient, σ not more than 0.9 whereby the effective membrane thickness, Δx was fixed at 150 μm [24, 40, 53].

Table 4 displayed the parameters and characteristics data of the prepared NF membranes. Generally, according to modeling studies the use of solutes with varying molecular weights often increased the reflection coefficient, σ and decreased the solute permeability, P_s. The percentage of smaller membrane pores compared to the molecules in the testing solution, enabling for an evaluation of the performance of the membrane, is represented by the value of σ. At the optimum polymer content, the NF21 membranes possess of pore radius, r_p and ratio of membrane thickness to porosity, $\Delta x/A_k$ are in the ranges of 0.96 to 1.37 nm and 4.96 to 98.29 μm, respectively. The smaller and good values of these properties were resulted in increment of salt rejection and good data in water flux. Although the increasing of polymer concentration produced smaller pore radius, the solute permeability and porosity factor were found to be very low. Moreover, at the optimum polymer concentration, the ratio of solute radius over pore radius, η shows good values from 0.19 to 0.82. In details analysis, the optimum polymer concentration produced of good ranges membranes parameters and fine properties which are very important and affected the separation performance and NF transport mechanism [54, 55].

Modeling results on the membranes parameters and properties showed that the polymer concentration played a significant roles determining of NF characteristics and separation performance. For further analysis, the impact of polymer content on the steric-hindrance factors of the fabricated membranes at different polymer concentration was summarized in Table 5.

Table 3 Membranes parameters and properties of skinned NF membranes at different PES concentration

Membranes	Neutral solutes	Membrane parameters and properties					
		σ (-)	r_p (nm)	η (r_s/r_p)	P_s (10^{-7} m/s)	A_k (-)	$\Delta x/A_k$ (μm)
	Glycerol	0.19	2.48	0.11	4.25	1.25	120.16
	Glucose	0.31	1.99	0.18	2.43	1.50	100.02
NF17	Saccharose	0.50	1.41	0.33	1.72	2.25	66.67
	Raffinose	0.59	1.39	0.42	1.38	2.96	50.73
	PEG 1000	0.81	1.15	0.68	0.62	9.81	15.29
	Glycerol	0.29	1.53	0.17	3.94	1.45	103.44
	Glucose	0.36	1.66	0.22	2.35	1.64	91.37
NF19	Saccharose	0.49	1.45	0.32	1.76	2.19	68.44
	Raffinose	0.61	1.33	0.44	1.22	3.18	47.23
	PEG 1000	0.86	1.04	0.75	0.38	16.58	9.05
	Glycerol	0.32	1.37	0.19	3.71	1.53	98.29
	Glucose	0.39	1.51	0.24	2.12	1.74	86.13
NF21	Saccharose	0.59	1.13	0.42	1.45	2.96	50.73
	Raffinose	0.71	1.06	0.55	0.92	4.95	30.32
	PEG 1000	0.90	0.96	0.82	0.21	30.25	4.96
	Glycerol	0.39	1.07	0.24	2.71	1.74	86.13
	Glucose	0.47	1.19	0.31	1.90	2.08	71.99
NF23	Saccharose	0.62	1.05	0.45	1.23	3.30	45.49
	Raffinose	0.75	0.97	0.60	0.78	6.25	24.00
	PEG 1000	0.93	0.90	0.86	0.12	58.41	2.57
	Glycerol	0.41	1.01	0.26	2.31	1.82	82.62
	Glucose	0.49	1.12	0.32	1.76	2.19	68.44
NF25	Saccharose	0.66	0.96	0.49	1.07	3.88	38.63
	Raffinose	0.78	0.91	0.64	0.66	7.69	19.51
	PEG 1000	0.94	0.88	0.89	0.09	78.03	1.92

Table 4 SHP parameters for skinned NF membranes at different PES concentration

Membrane parameters	PES concentration (wt%)				
	17	19	21	23	25
σ	0.03	0.04	0.12	0.14	0.15
H_F	1.03	1.04	1.13	1.16	1.17
S_F	0.94	0.92	0.78	0.74	0.73
S_D	0.76	0.72	0.53	0.49	0.48

Table 5 Properties of skinned NF membranes

Properties	PES concentration (wt%)				
	17	19	21	23	25
$P_s \times 10^{-7}$ (m/s)	3.32	3.41	2.49	1.97	1.82
$\Delta x/A_k$ (μm)	15.30	9.05	4.96	2.57	1.92
r_p (nm)	1.69	1.40	1.20	1.04	0.98
ζ (-)	1.04	1.10	1.56	1.67	1.71
X_d	0.017	0.018	0.027	0.028	0.029

The steric effects, S_F and S_D, were lowered as polymer concentration increased in terms of convection and diffusion factor. At the optimum polymer concentration, the membranes demonstrated of good values of steric-hindrance factors. In combination to a good value of reflection coefficient separation factor, σ = 0.12, these parameters and factors promoted the membranes for a good permeation, high selectivity and fine morphology. In accordance with the SHP model, these parameters greatly influenced the membrane transport mechanism for NF process [55].

In the membranes fabrication and characterization, the changing of membranes parameters and properties are very significant to the membranes separation performance. In order to analysis the fabrication and performance-properties of asymmetric NF membranes, full set of modeling data on membranes properties were determined and tabulated in Table 6. Modeling data of the electrostatic properties showed that the membrane surface charge density, X_d and zeta potential, ζ were increased at higher polymer concentration. At low polymer concentration (< 20 wt%) produced small values of electrical properties while the higher polymer concentration the higher values obtained. At the optimum polymer concentration, the membranes discovered to have surface charge density, X_d and zeta potential, ζ of about 0.027 and −1.56, respectively.

Table 6 Commercial NF vs skinned NF membranes

Properties	$\Delta x/A_k$ (μm)	r_p (nm)	ζ (-)
Minimum	0.66	0.39	1.5
Mean	4.8	0.66	9.2
Maximum	16.9	1.59	44.5
NF21	4.96*	1.20*	1.56*

* Mean values of modelling data

3.3 Morphologies and pore size distribution

Based on images analysis by Scanning Electron Microscopy (SEM) technique, different features of membranes pores and sublayer such as finger like, cellular, sponge like, nodular, compact/dense structure and tears like were found to be affected the membranes performances and separation characteristics. A dense and thicker skin layer was created as the polymer concentration in the casting solution increased, producing an asymmetric membrane that was more selective but less effective [55–57].

As the high concentration of polymer displayed thicker skin layers with highly porous substructure, the lower polymer produced thinner skin layers with large uniform voids across the substructure. The findings proved that the membranes performance and characteristics are depending to the features polymer solution and materials interactions and constituents [58, 59]. Fig. 6 showed the SEM images comprises of cross section structures and skin layers of skinned NF membranes at different PES concentration. These images depicted of asymmetrical structures as well as smooth and even top skin layer.

Based on the SEM images, the NF membranes structures composed of thinner active layer and highly porous finger like sublayer. As increment in polymer concentration, PES membrane frequently develops a thicker and denser skin layer. It showed similar cross sectional morphologies with very porous macrovoids. Fig. 6 (a)–(e) depicts that the length of the macrovoids decreased as the polymer concentration increased. At low polymer concentration, the membranes produced large macrovoid whereas a much smaller macrovoids was formed from high polymer concentration solution. However, at high polymer concentration (> 21 wt%), the NF membranes posed of a narrow like pores and spongy sublayer. The declined in flux and salt rejection are the result of minimal pores distribution and the suppression of macrovoid.

As a result, it was anticipated that the sublayer's demixing and precipitation processes would occur more slowly and resulted towards thick and dense skin layer in asymmetrical membranes [60, 61]. In addition, the casting solution's viscosity was raised by the addition of more polymers, producing membranes that were more selective but less productive [62]. The crucial parameter affecting properties-performance of membrane is the amount of polymer concentration, which directly impacts the viscosity of casting solution [63].

Cross sectional membranes analysis revealed that thicker skin layer thickness was produced at high polymer concentration. The formation of skinned macrovoids with

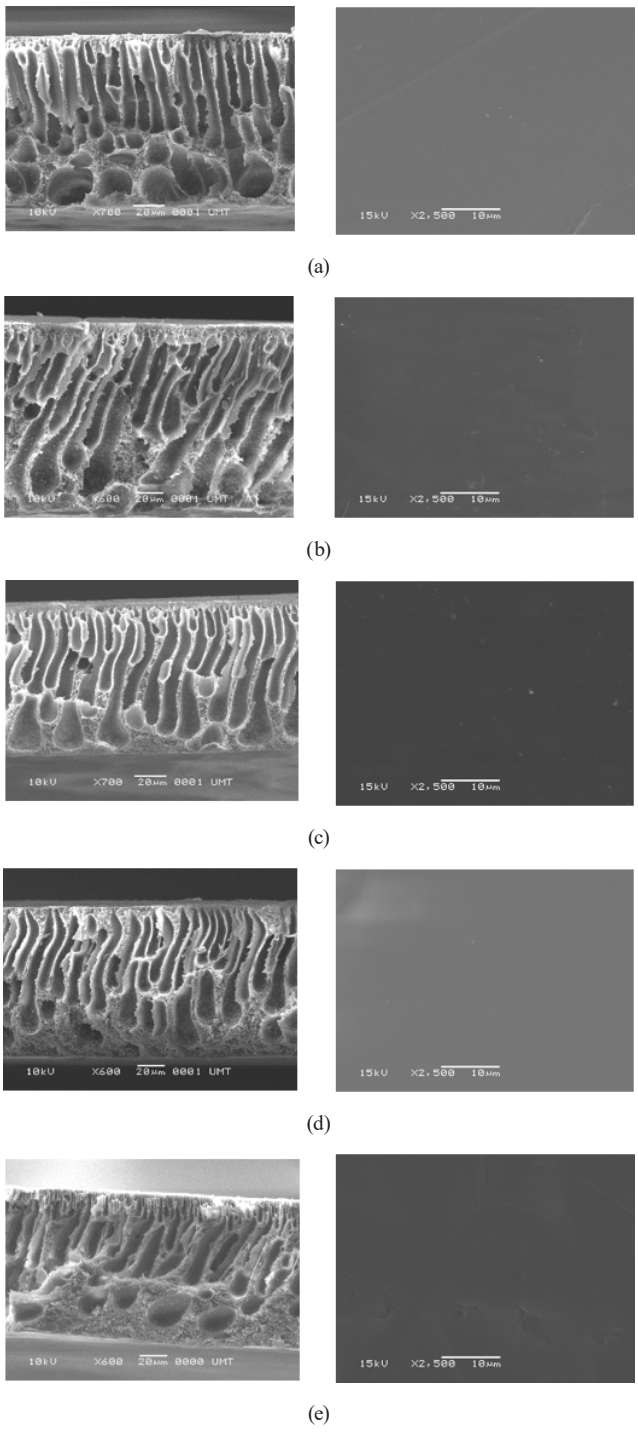

Fig. 6 Cross sectional structures and skin layers of skinned NF membranes of (a) NF17, (b) NF19, (c) NF21, (d) NF23 and (e) NF25

surrounded of thick dense layer instead of finger like structures resulted to a separation improvement. The formation of this skinned macrovoids maybe connected to a decline in demixing rates driven on by viscosity effects [64, 65]. Based on the results of solute rejection as represented in Table 4, solute transport method was employed for determination of pore size and pore size distribution (PSD) determination. The nature of membranes pore size distribution

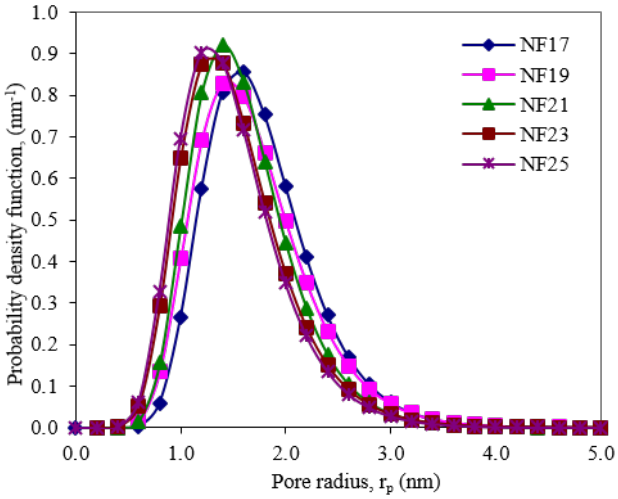

Fig. 7 PSD of skinned NF membranes determined by solute transport method using the data represented in Table 4

was examined based on method described by Bowen and Mohammad [66]. In terms of probability density function, the pore size distribution of skinned membranes with difference polymer concentration was depicted in Fig. 7.

From the graph, the membranes showed a good and narrow pore size distribution. It was revealed that at higher polymer concentration the narrower pore size distribution was produced. Hence, high polymer concentration (> 20 wt%) not only improved the membranes performances but also produced good membranes characteristics as well as the narrowest pore size distribution as reported by other researchers [9, 18, 32].

This finding also could be the significant reason of membranes performances profiles. Besides, the analysis result also support and prove that the polymer concentration played an important role determining of separation performance and membranes properties. Meanwhile, Fig. 7 showed the summary of NF membranes morphological structures-pore size distribution and morphological structures-key properties, respectively. Pore size distribution analysis and modeling results revealed that the NF21 membranes produced fine pore size distribution and key properties with 1.20 nm of pore radius, 4.96 μm of $\Delta x/A_k$ and −1.56 of surface charge, ζ, respectively. This data proved that the optimum polymer concentration for this study was found to be at 20.42 wt%.

4 Conclusions

The polymeric skinned asymmetric NF membranes were successfully developed. Analysis on the performances-properties showed that the increasing of polymer concentration in dope solution produced selective membranes. At an optimal PES concentration, the skinned NF

membranes possess of good performance, fine structural and key properties. The nanofiltration membranes produced at 20.42 wt% possess the narrow of pore radius and high surface charge of about 1.20 nm and 1.56 respectively. Based on modelling analysis, polymer concentrations factor was found to be significant and practical for the modification of membrane performance and properties. The findings from this study also proved that the manipulation of good membranes material is a good attempt to upgrade the membranes characteristics and efficacy which are potentially to be applied in specific applications such as in water treatment and wastewater treatment industries.

Acknowledgment

The authors gratefully acknowledge of ESERI and INOS for their assistance and advice.

Nomenclature

A	membrane area (m^2)
A_k	porosity (-)
c	concentrate (mol/m^3)
c_b	bulk concentration (mol/m^3)
c_p	permeate concentration (mol/m^3)
$c_{p,i}$	component i in the permeate (mol/m^3)
$c_{r,i}$	component i in the rejection (mol/m^3)
c_w	concentration of solute in the feed solution (mol/m^3)
D_∞	diffusion coefficient (m^2s)
F	Faraday constant (=96487) (C/mol)
H_D	hindrance diffusion parameters (-)
H_F	hindrance convection parameters (-)
J_s	solute flux (mol/m^2s)
J_v	volume flux (m/s)
M_w	molecular weight (g/mol)
P	permeability (m/s)
P_s	solute permeability (m/s)
r	radius of stirred cell
r_p	pore radius (nm)
r_s	stoke radius of solute (m)
R_{obs}	observation rejection (%)
R_{real}	real rejection (%)
S_D	steric diffusion parameter (-)
S_F	steric convection parameter (-)
Δt	time interval (s)
V	volume of permeate (m^3)
X_d	charge density (mol/m^3)
ΔP	Pressure (kPa)
Δx	membrane thickness (m)
$\Delta x/A_k$	membrane thickness over membrane porosity (μm)

Greek

σ	reflection coefficient/separation factor (-)
ε	porosity (-)
η	solute radius/pore radius (-)
τ	tortuosity (-)
ζ	zeta potential (-)

References

[1] Shahmirzadi, M. A. A., Hosseini, S. S., Ruan, G., Tan, N. R. "Tailoring PES nanofiltration membranes through systematic investigations of prominent design, fabrication and operational parameters", RSC Advances, 5(61), pp. 49080–49097, 2015. https://doi.org/10.1039/C5RA05985B

[2] Sadrzadeh, M., Bhattacharjee, S. "Rational design of phase inversion membranes by tailoring thermodynamics and kinetics of casting solution using polymer additives", Journal of Membrane Science, 441, pp. 31–44, 2013. https://doi.org/10.1016/j.memsci.2013.04.009

[3] Aroon, M. A., Ismail, A. F., Matsuura, T., Montazer-Rahmati, M. M. "Performance studies of mixed matrix membranes for gas separation: A review", Separation and Purification Technology, 75(3), pp. 229–242, 2010. https://doi.org/10.1016/j.seppur.2010.08.023

[4] Hołda, A. K., Vankelecom, I. F. J. "Understanding and guiding the phase inversion process for synthesis of solvent resistant nanofiltration membranes", Journal of Applied Polymer Science, 132(27), 42130, 2015. https://doi.org/10.1002/app.42130

[5] Ali, N. S. M., Hassan, A. R. "The effect of CTAB and SDS surfactant on the morphology and performance of low pressure active reverse osmosis membrane", Malaysian Journal of Analytical Science, 20(3), pp. 510–516, 2016. https://doi.org/10.17576/mjas-2016-2003-07

[6] Singh, R. "Chapter 1 - Introduction to membrane technology", In: Membrane Technology and Engineering for Water Purification, Butterworth-Heinemann, 2015, pp. 1–80. ISBN 978-0-444-63362-0 https://doi.org/10.1016/B978-0-444-63362-0.00001-X

[7] Purkait, M. K., Sinha, M. K., Mondal, P., Singh, R. "Chapter 1 - Introduction to membranes", Interface Science And Technology, 25, pp. 1–37, 2018. https://doi.org/10.1016/B978-0-12-813961-5.00001-2

[8] Safari, N. H. M., Hassan, A. R., Che Wan Takwa, C. W. I., Rozali, S. "Deduction of Surfactants Effect on Performance, Morphology, Thermal and Molecular Properties of Polymeric Polyvinylidene Fluoride (PVDF) Based Ultrafiltration Membrane", Periodica Polytechnica Chemical Engineering, 63(1), pp. 27–35, 2019. https://doi.org/10.3311/PPch.12423

[9] Safari, N. H. M., Rozali, S., Hassan, A. R., Ahmad, M. "Tailoring of Narrow Pores, Pore Size Distribution and Structural Details in Asymmetric Nanofiltration Membranes via Polyvinyl-pyrrolidone Additive", Periodica Polytechnica Chemical Engineering, 66(4), pp. 576–584, 2022. https://doi.org/10.3311/PPch.19805

[10] Alibakhshi, S., Youssefi, M., Hosseini, S. S., Zadhoush, A. "Tuning morphology and transport in ultrafiltration membranes derived from polyethersulfone through exploration of dope formulation and characteristics", Materials Research Express, 6(12), 125326, 2019. https://doi.org/10.1088/2053-1591/ab56c3

[11] Bagheripour, E., Moghadassi, A. R., Parvizian, F., Hosseini, S. M., Van der Bruggen, B. "Tailoring the separation performance and fouling reduction of PES based nanofiltration membrane by using a PVA/Fe_3O_4 coating layer", Chemical Engineering Research and Design, 144, pp. 418–428, 2019. https://doi.org/10.1016/j.cherd.2019.02.028

[12] Zhou, C., Hou, Z., Lu, X., Liu, Z., Bian, X., Shi, L., Li, L. "Effect of polyethersulfone molecular weight on structure and performance of ultrafiltration membranes", Industrial & Engineering Chemistry Research, 49(20), pp. 9988–9997, 2010. https://doi.org/10.1021/ie100199h

[13] Irfan, M., Idris, A., Yusof, N. M., Khairuddin, N. F. M., Akhmal, H. "Surface modification and performance enhancement of nano-hybrid f-MWCNT/PVP90/PES hemodialysis membranes", Journal of Membrane Science, 467, pp. 73–84, 2014. https://doi.org/10.1016/j.memsci.2014.05.001

[14] Zhao, Y.-F., Zhu, L.-P., Yi, Z., Zhu, B.-K., Xu, Y. "Improving the hydrophilicity and fouling-resistance of polysulfone ultrafiltration membranes via surface zwitterionicalization mediated by polysulfone-based triblock copolymer additive", Journal of Membrane Science, 440, pp. 40–47, 2013. https://doi.org/10.1016/j.memsci.2013.03.064

[15] Hilal, N., Al-Zoubi, H., Darwish, N. A., Mohammad, A. W., Arabi, M. A. "A comprehensive review of nanofiltration membranes: Treatment, pretreatment, modelling, and atomic force microscopy", Desalination, 170(3), pp. 281–308, 2004. https://doi.org/10.1016/j.desal.2004.01.007

[16] Tofighy, M. A., Mohammadi, T., Sadeghi, M. H. "High-flux PVDF/PVP nanocomposite ultrafiltration membrane incorporated with graphene oxide nanoribbones with improved antifouling properties", Journal of Applied Polymer Science, 138(4), 49718, 2021. https://doi.org/10.1002/app.49718

[17] Lee, A., Elam, J. W., Darling, S. B. "Membrane materials for water purification: design, development, and application", Environmental Science: Water Research & Technology, 2(1), pp. 17–42, 2016. https://doi.org/10.1039/C5EW00159E

[18] Hassan, A. R., Abdul Munaim, M. S. "Fabrication and characterization of integrally skinned-oriented highly selective charged asymmetric low pressure poly(ether sulfone) membranes for nanofiltration", Journal of Chemical Technology and Biotechnology, 87(4), pp. 559–569, 2012. https://doi.org/10.1002/jctb.2751

[19] Tavangar, T., Karimi, M., Rezakazemi, M., Reddy, K. R., Aminabhavi, T. M. "Textile waste, dyes/inorganic salts separation of cerium oxide-loaded loose nanofiltration polyethersulfone membranes", Chemical Engineering Journal, 385, 123787, 2020. https://doi.org/10.1016/j.cej.2019.123787

[20] Long, Q., Zhang, Z., Qi, G., Wang, Z., Chen, Y., Liu, Z.-Q. "Fabrication of chitosan nanofiltration membranes by the film casting strategy for effective removal of dyes/salts in textile wastewater", ACS Sustainable Chemical & Engineering, 8(6), pp. 2512–2522, 2020. https://doi.org/10.1021/acssuschemeng.9b07026

[21] Hidayah, M., Kusworo, T. D., Susanto, H. "Improving the Performance of Polysulfone-nano ZnO Membranes for Water Treatment in Oil Refinery with Modified UV Irradiation and Polyvinyl Alcohol", Periodica Polytechnica Chemical Engineering, 66(1), pp. 43–53, 2022. https://doi.org/10.3311/PPch.17029

[22] Alsobh, A., Zin, M. M., Vatai, G., Bánvölgyi, S. "The Application of Membrane Technology in the Concentration and Purification of Plant Extracts: A Review", Periodica Polytechnica Chemical Engineering, 66(3), pp. 394–408, 2022. https://doi.org/10.3311/PPch.19487

[23] Wu, F., Feng, L., Zhang, L. "Rejection prediction of isopropylantipyrine and antipyrine by nanofiltration membranes based on the Spiegler–Kedem–Katchalsky model", Desalination, 362, pp. 11–17, 2015. https://doi.org/10.1016/j.desal.2015.01.046

[24] Hassan, A. R., Ali, N., Abdull, N., Ismail, A. F. "A theoretical approach on membrane characterization: the deduction of fine structural details of asymmetric nanofiltration membranes", Desalination, 206(1–3), pp. 107–126, 2007. https://doi.org/10.1016/j.desal.2006.06.008

[25] Jain, S., Gupta, S. K. "Analysis of modified suface pore flow model with concentration polarization and comparison with Spiegler–Kedem model in reverse osmosis system", Journal of Membrane Science, 232(1–2), pp. 45–62, 2004. https://doi.org/10.1016/j.memsci.2003.11.021

[26] Rozali, S., Safari, N. H. M., Hassan, A. R., Ahmad, M., Yunus, R. M. "Assessment on Performance-properties of Asymmetric Nanofiltration Membranes from Polyethersulfone/n-Methyl-2-pyrrolidone/water Blends with Poly(vinyl pyrrolidone) as Additive", Periodica Polytechnica Chemical Engineering, 66(1), pp. 54–69, 2022. https://doi.org/10.3311/PPch.18357

[27] Safari, N. H. M., Rozali, S., Hassan, A. R., Osman, R. "Inducing the skinned-oriented asymmetrical nanofiltration membranes via controlled evaporation times in dry/wet phase inversion process", Applied Science and Engineering Progress, 16(2), 6015, 2023. https://doi.org/10.14416/j.asep.2022.05.007

[28] Siddiqui, M. U., Arif, A. F. M., Bashmal, S. "Permeability-selectivity analysis of microfiltration and ultrafiltration membranes: Effect of pore size and shape distribution and membrane stretching", Membranes, 6(3), 40, 2016. https://doi.org/10.3390/membranes6030040

[29] Shang, W.-J., Tu, C.-H., Wang, X.-L. "Theoretical calculation of reflection coefficients of single salt solutions through charged porous membranes", Desalination, 236(1–3), pp. 306–315, 2009. https://doi.org/10.1016/j.desal.2007.10.081

[30] Sapalidis, A. A. "Porous polyvinyl alcohol membranes: preparation methods and applications", Symmetry, 12(6), 960, 2020. https://doi.org/10.3390/sym12060960

[31] Ji, Y.-L., Gu, B.-X., An, Q.-F., Gao, C.-J. "Recent advances in the fabrication of membranes containing "ion pairs" for nanofiltration processes", Polymers, 9(12), 715, 2017. https://doi.org/10.3390/polym9120715

[32] Mustaffar, M. I., Ismail, A. F., Illias, R. M. "Study on the effect of polymer concentration on hollow fiber ultrafiltration membrane performance and morphology", presented at Regional Symposium on Membrane Science and Technology, Johor Bahru, Malaysia, Apr. 21–25, 2004.

[33] Tang, Y.-H., Ledieu, E. Cervellere, M. R., Millett, P. C., Ford, D. M., Qian, X. "Formation of polyethersulfone membranes via non-solvent induced phase separation process from dissipative particle dynamics simulations", Journal of Membrane Science, 599, 117826, 2020. https://doi.org/10.1016/j.memsci.2020.117826

[34] Dahe, G. J., Singh, R. P., Dudeck, K. W., Yang, D., Berchtold, K. A. "Influence of non-solvent chemistry on polybenzimidazole hollow fiber membrane preparation", Journal of Membrane Science, 577, pp. 91–103, 2019. https://doi.org/10.1016/j.memsci.2019.02.001

[35] Epsztein, R., Shaulsky, E., Dizge, N., Warsinger, D. M., Elimelech, M. "Role of ionic charge density in Donnan exclusion of monovalent anions by nanofiltration", Environmental Science & Technology, 52(7), pp. 4108–4116, 2018. https://doi.org/10.1021/acs.est.7b06400

[36] Nakao, S., Kimura, S. "Models of membrane transport phenomena and their applications for ultrafiltration data", Journal of Chemical Engineering of Japan, 15(3), pp. 200–205, 1982. https://doi.org/10.1252/jcej.15.200

[37] MiniTAB, LLC. "MiniTAB®, (17.10)", [computer program] Available at: https://www.minitab.com/en-us/products/minitab [Accessed: 10 December 2022]

[38] Pisano, A. "From tubes and catheters to the basis of hemodynamics: Viscosity and Hagen–Poiseuille equation", In: Physics for Anesthesiologists and Intensivists, Springer, pp. 89–98, 2021. ISBN 978-3-030-72046-9 https://doi.org/10.1007/978-3-030-72047-6_8

[39] Roy, Y., Lienhard, J. H. "On the presence of solute-solvent transport coupling in reverse osmosis", Journal of Membrane Science, 611, 118272, 2020. https://doi.org/10.1016/j.memsci.2020.118272

[40] Ismail, A. F., Hassan, A. R. "Effect of additive contents on the performances and structural properties of asymmetric polyethersulfone (PES) nanofiltration membranes", Separation and Purification Technology, 55(1), pp. 98–109, 2007. https://doi.org/10.1016/j.seppur.2006.11.002

[41] Agboola, O., Maree, J., Kolesnikov, A., Mbaya, R., Sadiku, R. "Theoretical performance of nanofiltration membranes for wastewater treatment", Environmental Chemistry Letters, 13(1), pp. 37–47, 2015. https://doi.org/10.1007/s10311-014-0486-y

[42] Maruf, S. H., Li, Z., Yoshimura, J. A., Xiao, J., Greenberg, A. R., Ding, Y. "Influence of nanoimprint lithography on membrane structure and performance", Polymer, 69, pp. 129–137, 2015. https://doi.org/10.1016/j.polymer.2015.05.049

[43] Xu, R., Zhou, M., Wang, H., Wang, X., Wen, X. "Influences of temperature on the retention of PPCPs by nanofiltration membranes: Experiments and modeling assessment", Journal of Membrane Science, 599, 117817, 2020. https://doi.org/10.1016/j.memsci.2020.117817

[44] Manzano, I., Zydney, A. L. "Quantitative study of RNA transmission through ultrafiltration membranes", Journal of Membrane Science, 544, pp. 272–277, 2017. https://doi.org/10.1016/j.memsci.2017.09.042

[45] Wang, X.-L., Wang, W.-N., Wang, D.-X. "Experimental investigation on separation performance of nanofiltration membranes for inorganic electrolytes solutions", Desalination, 145(1–3), pp. 115–122, 2002. https://doi.org/10.1016/S0011-9164(02)00395-8

[46] Szymczyk, A., Labbez, C., Fievet, P., Vidonne, A., Foissy, A., Pagetti, J. "Contribution of convection, diffusion and migration to electrolyte transport through nanofiltration membranes", Advances in Colloid and Interface Science, 103(1), pp. 77–94, 2003. https://doi.org/10.1016/S0001-8686(02)00094-5

[47] Labbez, C., Fievet, P., Szymczyk, A., Vidonne, A., Foissy, A., Pagetti, J. "Retention of mineral salts by a polyamide nanofiltration membrane", Separation and Purification Technology, 30(1), pp. 47–55, 2003. https://doi.org/10.1016/S1383-5866(02)00107-7

[48] Chung, T. S., Teoh, S. K., Hu, X. "Formation of ultrathin high-performance polyethersulfone hollow-fiber membranes", Journal of Membrane Science, 133(2), pp. 161–175, 1997. https://doi.org/10.1016/S0376-7388(97)00101-4

[49] Kamcev, J., Galizia, M., Benedetti, F. M., Jang, E.-S., Paul, D. R., Freeman, B. D., Manning, G. S. "Partitioning of mobile ions between ion exchange polymers and aqueous salt solutions: importance of counter-ion condensation", Physical Chemistry Chemical Physics, 18(8), pp. 6021–6031, 2016. https://doi.org/10.1039/C5CP06747B

[50] Liu, G., Ye, H., Li, A., Zhu, C., Jiang, H., Liu, Y., Han, K., Zhou, Y. "Graphene oxide for high-efficiency separation membranes: Role of electrostatic interactions", Carbon, 110, pp. 56–61, 2016. https://doi.org/10.1016/j.carbon.2016.09.005

[51] Liang, Y., Lin, S. "Mechanism of permselectivity enhancement in polyelectrolyte-dense nanofiltration membranes via surfactant-assembly intercalation", Environmental Science & Technology, 55(1), pp. 738–748, 2021. https://doi.org/10.1021/acs.est.0c06866

[52] Ladewig, B., Al-Shaeli, M. N. Z. "Fundamentals of membrane processes", In: Fundamentals of Membrane Bioreactors: Materials, Systems and Membrane Fouling, Springer, 2017, pp. 13–37. ISBN 978-981-10-2013-1 https://doi.org/10.1007/978-981-10-2014-8_2

[53] Wang, X.-L., Tsuru, T., Nakao, S., Kimura, S. "The electrostatic and steric-hindrance model for the transport of charged solutes through nanofiltration membranes", Journal of Membrane Science, 135(1), pp. 19–32, 1997. https://doi.org/10.1016/S0376-7388(97)00125-7

[54] Chen, X., Tang, B., Luo, J., Wan, Y. "Towards high-performance polysulfone membrane: The role of PSF-b-PEG copolymer additive", Microporous and Mesoporous Materials, 241, pp. 355–365, 2017.
https://doi.org/10.1016/j.micromeso.2016.12.032

[55] Gebru, K. A., Das, C. "Effects of solubility parameter differences among PEG, PVP and CA on the preparation of ultrafiltration membranes: Impacts of solvents and additives on morphology, permeability and fouling performances", Chinese Journal of Chemical Engineering, 25(7), pp. 911–923, 2017.
https://doi.org/10.1016/j.cjche.2016.11.017

[56] Zainal, S. H., Hassan, A. R., Isa, M. H. M. "The effect of polymer concentration and surfactant types on nanofiltration-surfactant membrane for textile wastewater", Malaysian Journal of Analytical Sciences, 20(6), pp. 1524–1529, 2016.
https://doi.org/10.17576/mjas-2016-2006-34

[57] Otero-Fernández, A., Otero, J. A., Maroto, A., Carmona, J., Palacio, L., Prádanos P., Hernández, A. "Concentration-polarization in nanofiltration of low concentration Cr(VI) aqueous solutions. Effect of operative conditions on retention", Journal of Cleaner Production, 150, pp. 243–252, 2017.
https://doi.org/10.1016/j.jclepro.2017.03.014

[58] Hassan, A. R., Rozali, S., Safari, N. H. M., Besar, B. H. "The roles of polyethersulfone and polyethylene glycol additive on nanofiltration of dyes and membrane morphologies", Environmental Engineering Research, 23(3), pp. 316–322, 2018.
https://doi.org/10.4491/eer.2018.023

[59] Sulaiman, N. A., Hassan, A. R., Rozali, S., Mohd Safari, N. H., Takwa, C. W. I. C. W., Mansoor A, A. D. K., Md Saad, M. H. "Development of Asymmetric Low Pressure Reverse Osmosis-Surfactants Membrane: Effect of Surfactant Types and Concentration", Periodica Polytechnica Chemical Engineering, 64(3), pp. 296–303, 2020.
https://doi.org/10.3311/PPch.13327

[60] Mazinani, S., Darvishmanesh, S., Ehsanzadeh, A., Van der Bruggen, B. "Phase separation analysis of Extem/solvent/non-solvent systems and relation with membrane morphology", Journal of Membrane Science, 526, pp. 301–314, 2017.
https://doi.org/10.1016/j.memsci.2016.12.031

[61] Hassan, A. R., Che Wan Takwa, C. W. I., Mohd Safari, N. H., Rozali, S., Sulaiman, N. A. "Characterization on Performance, Morphologies and Molecular Properties of Dual-Surfactants Based Polyvinylidene Fluoride Ultrafiltration Membranes", Periodica Polytechnica Chemical Engineering, 64(3), pp. 320–327, 2020.
https://doi.org/10.3311/PPch.13862

[62] Pesek, S. C., Koros, W. J. "Aqueous quenched asymmetric polysulphone hollow fibers prepared by dry/wet phase separation", Journal of Membrane Science, 88(1), pp. 1–19, 1994.
https://doi.org/10.1016/0376-7388(93)E0150-I

[63] Ali, I., Bamaga, O. A., Gzara, L., Bassyouni, M., Abdel-Aziz, M. H., Soliman, M. F., Drioli, E., Albeirutty, M. "Assessment of blend PVDF membranes, and the effect of polymer concentration and blend composition", Membranes, 8(1), 13, 2018.
https://doi.org/10.3390/membranes8010013

[64] Luque-Alled, J. M., Abdel-Karim, A., Alberto, M., Leaper, S., Perez-Page, M., Huang, K., Vijayaraghavan, A., El-Kalliny, A. S., Holmes, S. M., Gorgojo, P. "Polyethersulfone membranes: From ultrafiltration to nanofiltration via the incorporation of APTS functionalized-graphene oxide", Separation and Purification Technology, 230, 115836, 2020.
https://doi.org/10.1016/j.seppur.2019.115836

[65] Alhweij, H., Emanuelsson, E. A. C., Shahid, S., Wenk, J. "Simplified in-situ tailoring of cross-linked self-doped sulfonated polyaniline (S-PANI) membranes for nanofiltration applications", Journal of Membrane Science, 637, 119654, 2021.
https://doi.org/10.1016/j.memsci.2021.119654

[66] Bowen, W. R., Mohammad, A. W. "Characterization and prediction of nanofiltration membrane performance—a general assessment", Chemical Engineering Research and Design, 76(8), pp. 885–893, 1998.
https://doi.org/10.1205/026387698525685